Incremental Diagnostic Benefit of Superparamagnetic Iron Oxides-Enhanced 2D Gradient Echo Images Compared to Double-Contrast 3D Gradient Echo Images for Hepatocellular Carcinoma Detection

S. W. Kwan[1], D. A. Aguirre[2], A. Santosa[2], C. B. Sirlin[2]

[1]Department of Radiology, Stanford University School of Medicine, Stanford, CA, United States, [2]Department of Radiology, University of California at San Diego, San Diego, CA, United States

Introduction: The use of contrast-enhanced magnetic resonance (MR) has been shown to improve the detection of hepatocellular carcinoma (HCC). Multiple strategies have been employed, including the use of dynamic gadolinium (Gd)-based agents, superparamagnetic iron oxides (SPIO), or both. Prior studies have compared the diagnostic performance of Gd-enhanced vs. SPIO-enhanced images [1, 2], while others have explored the performance of double-contrast enhanced images [3, 4]. To our knowledge, no previous study has assessed the incremental benefit of SPIO-enhanced images used in conjunction with double-contrast enhanced images. The purpose of this study was to test our hypothesis that addition of SPIO-enhanced 2D gradient echo (GRE) images increases diagnostic accuracy for HCC detection in cirrhotic patients compared to double-contrast enhanced 3D GRE images only.

Materials & Methods: Two blinded abdominal radiologists retrospectively reviewed 60 double-contrast enhanced MR examinations of the liver. Examinations were performed with phased array coils at 1.5T and included:

(1) SPIO-enhanced, contiguous, 8-mm thick, 2D GREs (TR ≈ 150 ms, TEs of 2.4, 4.8 and 6.6ms; flip angle = 70^o);

(2) double-contrast enhanced, contiguous, 3-mm thick, spoiled 3D GREs (TR/TE/flip angle = 4.5/1.5/15^o) performed before and dynamically after bolus injection of an extracellular Gd-chelate timed to coincide with the hepatic arterial, portal venous, and equilibrium phases.

The study group included 30 patients with 54 pathology-confirmed HCCs (mean size, 25mm; range, 11-74mm) and 30 controls; all patients had pathology-confirmed cirrhosis. Reader A and B had 6 months and 3 years of experience reading SPIO-enhanced MR, respectively. A 5-point confidence score was given for the presence of HCC in each liver segment on the double-contrast enhanced 3D GREs. After reviewing the SPIO-enhanced 2D GREs in conjunction with the double-contrast enhanced GREs, a second score was given, using the same scale. The time taken to interpret each image set was recorded. Receiver-operating characteristics curves for the two scores were compared (paired comparison). Sensitivity, specificity, positive predictive value (PPV), negative predictive value (NPV), and likelihood ratios were calculated for each threshold score.

Results: For lesion detection, area under the curve (AUC) for Reader A using double-contrast 3D GREs was 0.863 (95% CI, 0.845-0.881) whereas AUC using both double-contrast and SPIO-enhanced GREs in conjunction was 0.886 (95% CI, 0.869-0.903) (p=0.22). AUC for Reader B using double-contrast GREs was 0.941 (95% CI, 0.928-0.953) whereas AUC using both image sets in conjunction was 0.973 (95% CI, 0.965-0.982) (p=0.12). For patient diagnosis, AUC for Reader A using double-contrast GREs was 0.881 (95% CI, 0.788-.974) whereas AUC using both image sets in conjunction was 0.939 (95% CI, 0.868-1.011) (p=0.15). For patient diagnosis, AUC for Reader B using double-contrast GREs was 0.929 (95% CI, 0.859-0.998) whereas AUC for both image sets in conjunction was 0.955 (95% CI, 0.896-1.014) (p=0.43).

At the optimal decision threshold, sensitivity/specificity for lesion detection increased from 67.9%/97.6% to 77.6%/98.1% for Reader A and from 79.2%/98.8% to 90.6%/99.0% for Reader B. PPV/NPV increased from 78.3%/96.0% to 83.7%/97.1% for Reader A and from 89.4%/97.4% to 92.3%/98.8%. Likelihood ratio positive increased from 28.2 to 40.1 for Reader A and from 65.8 to 93.4 for Reader B. Likelihood ratio negative decreased from 0.33 to 0.23 for Reader A and from 0.21 to 0.10 for Reader B.

The mean interpretation time for double-contrast 3D GREs was similar for Reader A (mean, 118s; SD, 41s) and Reader B (mean, 127s; SD, 64) (p=.28). In contrast, Reader B (mean, 113s; SD, 81s) took significantly longer to review both image sets in conjunction than Reader A (mean, 88s; SD, 54s) (p=.015).

Conclusions: The addition of SPIO-enhanced GRE images provided a clinically meaningful improvement in diagnostic performance. The degree to which the SPIO-enhanced GRE images improved performance may reflect reader experience with or time taken for interpreting SPIO-enhanced images. Based on the results of this study, we conclude that review of SPIO-enhanced 2D GRE images in conjunction with double-contrast enhanced 3D GRE images improves HCC detection in cirrhotic patients compared to review of double-contrast enhanced 3D GRE images alone.

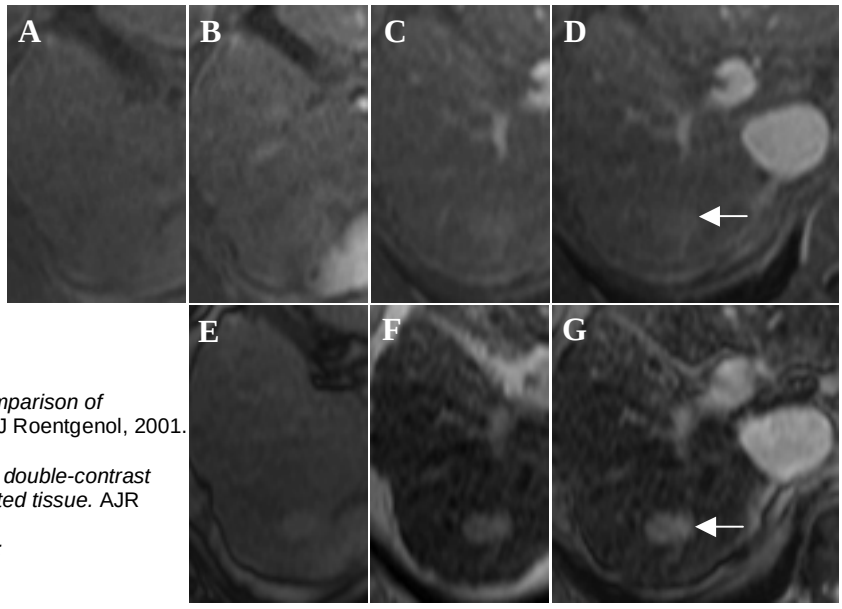

Figure 1. A-D: Pathology-confirmed 21mm HCC missed by both readers on double-contrast enhanced 3D GREs. A. Pre-contrast B. Arterial phase C. Portal-venous phase D. Equilibrium phase. E-G: Addition of SPIO-enhanced 2D GREs caused both readers to change their score to the highest confidence for malignancy. E. TE=2.4ms F. TE=4.8ms G.TE=6.6ms

References:

1. Pauleit, D., et al., *Hepatocellular carcinoma: detection with gadolinium- and ferumoxides-enhanced MR imaging of the liver.* Radiology, 2002. **222**(1): p. 73-80.
2. Matsuo, M., et al., *Detection of malignant hepatic tumors: comparison of gadolinium-and ferumoxide-enhanced MR imaging.* AJR Am J Roentgenol, 2001. **177**(3): p. 637-43.
3. Bhartia, B., et al., *Hepatocellular carcinoma in cirrhotic livers: double-contrast thin-section MR imaging with pathologic correlation of explanted tissue.* AJR Am J Roentgenol, 2003. **180**(3): p. 577-84.
4. Ward, J., et al., *Hepatocellular carcinoma in the cirrhotic liver: double-contrast MR imaging for diagnosis.* Radiology, 2000. **216**(1): p. 154-62.